Biochimica et Biophysica Acta 1798 (2010) 966–974

Contents lists available at ScienceDirect

Biochimica et Biophysica Acta

journal homepage: www.elsevier.com/locate/bbamem

Role of glycine residues highly conserved in the S2–S3 linkers of domains I and II of voltage-gated calcium channel α_1 subunits

Jinfeng Teng [a,e], Kazuko Iida [b], Masanori Ito [c,d], Hiroko Izumi-Nakaseko [c,d], Itaru Kojima [e], Satomi Adachi-Akahane [c,d,*], Hidetoshi Iida [a,f,*]

[a] Department of Biology, Tokyo Gakugei University, 4-1-1 Nukui kita-machi, Koganei-shi, Tokyo 184-8501, Japan
[b] Biomembrane Signaling Project 2, Tokyo Metropolitan Institute of Medical Science, 3-18-22 Honkomagome, Bunkyo-ku, Tokyo 113-8613, Japan
[c] Department of Pharmacology, School of Medicine, Faculty of Medicine, Toho University, 5-21-16 Omori-Nishi, Ota-ku, Tokyo 143-8540, Japan
[d] Advanced Medical Research Center, Toho University, 5-21-16 Omori-Nishi, Ota-ku, Tokyo 143-8540, Japan
[e] Laboratory of Cell Biology, Institute for Molecular and Cellular Regulation, Gunma University, Maebashi, Gunma 371-8510, Japan
[f] Department of Bioenvironmental Science, Okazaki Institute for Integrative Bioscience, National Institutes of Natural Sciences, Higashiyama 5-1, Myodaiji, Okazaki, Aichi 444-8787, Japan

ARTICLE INFO

Article history:
Received 21 October 2009
Received in revised form 19 December 2009
Accepted 4 January 2010
Available online 11 January 2010

Keywords:
Ca^{2+} channel
VGCC
VDCC
$Ca_v1.2$
S2–S3 linker
Glycine residue

ABSTRACT

The pore-forming component of voltage-gated calcium channels, α_1 subunit, contains four structurally conserved domains (I–IV), each of which contains six transmembrane segments (S1–S6). We have shown previously that a Gly residue in the S2–S3 linker of domain III is completely conserved from yeasts to humans and important for channel activity. The Gly residues in the S2–S3 linkers of domains I and II, which correspond positionally to the Gly in the S2–S3 linker of domain III, are also highly conserved. Here, we investigated the role of the Gly residues in the S2–S3 linkers of domains I and II of $Ca_v1.2$. Each of the Gly residues was replaced with Glu or Gln to produce mutant $Ca_v1.2$s; G182E, G182Q, G579E, G579Q, and the resulting mutants were transfected into BHK6 cells. Whole-cell patch-clamp recordings showed that current–voltage relationships of the four mutants were the same as those of wild-type $Ca_v1.2$. However, G182E and G182Q showed significantly smaller current densities because of mislocalization of the mutant proteins, suggesting that Gly^{182} in domain I is involved in the membrane trafficking or surface expression of α_1 subunit. On the other hand, G579E showed a slower voltage-dependent current inactivation (VDI) compared to $Ca_v1.2$, although G579Q showed a normal VDI, implying that Gly^{579} in domain II is involved in the regulation of VDI and that the incorporation of a negative charge alters the VDI kinetics. Our findings indicate that the two conserved Gly residues are important for α_1 subunit to become functional.

1. Introduction

Voltage-gated calcium channels (VGCCs) regulate Ca^{2+} influx required for various cellular functions, including muscle contraction, neurotransmitter release, and gene expression [1]. VGCCs are composed minimally of α_1, β, and α_2/δ subunits [2]. α_1 subunit is the major voltage-sensitive and pore-forming component of VGCCs and contains four structurally conserved domains (I–IV). Each domain contains six transmembrane segments (S1–S6) and a membrane-associated loop between the S5 and S6 segments (called the P-loop). The S4 segments form the voltage sensor and P-loops form the Ca^{2+}-selective pore (see Fig. 1A).

The auxiliary subunits, β and α_2/δ, play prominent roles in the functional expression of α_1 subunits and in the regulation of channel function, including increases in current density as well as activation and inactivation of the channel [3]. In particular, it is proposed that β subunits bind to the α_1-interaction domain (AID) within the cytoplasmic I–II linker region and is crucial for the functional regulation of α_1 subunits [4,5]. Crystal structural analysis has shown that β subunits contain multiple protein-interacting modules, suggesting it to be a multi-functional protein [6]. In addition to these auxiliary subunits, several molecules such as G proteins and synaptic proteins have been reported to be involved in the function and surface expression of α_1 subunits [3]. It has been speculated that cytoplasmic regions of α_1 subunits, including N-terminal and C-terminal regions and linkers between the domains, constitute the binding/recognition sites for the auxiliary subunits and second messengers. Although a number of regions in α_1 subunits important for interaction with auxiliary subunits or regulatory molecules have been identified [4,7–10], little is known about the molecular mechanisms underlying the

Abbreviations: VGCC, voltage-gated Ca^{2+} channel; AID, α_1-interaction domain; VDI, voltage-dependent inactivation; CDI, Ca^{2+}-dependent inactivation

* Corresponding authors. S. Adachi-Akahane is to be contacted at Department of Pharmacology, School of Medicine, Faculty of Medicine, Toho University, 5-21-16 Omori-Nishi, Ota-ku, Tokyo 143-8540, Japan. Tel.: +81 3 3762 4151x2361; fax: +81 3 5493 5413. H. Iida, Department of Biology, Tokyo Gakugei University, 4-1-1 Nukui kita-machi, Koganei-shi, Tokyo 184-8501, Japan. Tel./fax: +81 42 329 7517.
E-mail addresses: satomiaa@med.toho-u.ac.jp (S. Adachi-Akahane), iida@u-gakugei.ac.jp (H. Iida).

0005-2736/$ – see front matter © 2010 Elsevier B.V. All rights reserved.
doi:10.1016/j.bbamem.2010.01.004

surface expression and the functional regulation of α_1 subunits from a structural point of view.

Previously, we have revealed that the Gly residue in the S2–S3 linker of domain III is completely conserved in the VGCC family from yeasts to humans and bears essential roles in the maintenance of channel activity [11]. Here, we show that the Gly residues in the S2–S3 linkers of domains I and II, which correspond positionally to the Gly residue in the S2–S3 linker of domain III, are also highly conserved during evolution. $Ca_v1.2$ is a member of the L-type VGCC α_1 subunit family, and its activity was successfully analyzed following transfection of its cDNA into baby hamster kidney BHK6 cells expressing rabbit β_{1a} and α_2/δ_1 subunits. In this study, we employed this cell line to investigate the roles of the two conserved Gly residues (Gly^{182} and Gly^{579} in $Ca_v1.2$). We found that the substitution of Glu or Gln for Gly^{182} resulted in a loss or reduction of peak current density because of the mislocalization of the mutant proteins, suggesting that the Gly^{182} residue in the S2–S3 linker of domain I is involved in the surface expression of the α_1 subunit. The substitution of the negatively charged Glu for Gly^{579} slowed voltage-dependent current inactivation (VDI), though no such effect was observed upon substitution of the uncharged Gln for Gly^{579}, indicating that Gly^{579} in the S2–S3 linker of domain II is involved in the regulation of the gating kinetics of $Ca_V1.2$. Our findings indicate that the conserved Gly residues in the S2–S3 linkers of domains I and II play important roles in maintaining the function of VGCCs.

2. Materials and methods

2.1. In vitro site-directed mutagenesis in $Ca_v1.2$ cDNA

In vitro site-directed mutagenesis was carried out on the cDNA of a rat brain $Ca_v1.2$, rbCII, which had been subcloned into pBluescript II SK(−) using the KOD-Plus-Mutagenesis Kit (Toyobo, Co., Osaka). The 1.3 kb KpnI–XhoI fragment or the 1.6 kb XhoI–SpeI fragment of the cDNA was replaced with a sequence-verified DNA fragment mutated at the position of the Gly^{182} or Gly^{579} residue of $Ca_v1.2$ and each full-length cDNA carrying the site-directed mutations was then introduced into pBCMS-EGFP as described previously [11].

2.2. Cell culture

BHK6 cells stably expressing rabbit β and α_2/δ_1 subunits [12] were cultured in Dulbecco's modified Eagle's medium supplemented with 5% fetal bovine serum, 100 U/ml of penicillin–streptomycin (Sigma) and 600 μg/ml of G418 in a humidified 5% CO_2/95% O_2 incubator at 37 °C [13]. Cells were plated on coverslips coated with 0.5% gelatin and transfected with a plasmid bearing $Ca_v1.2$ cDNA or its mutants using Fugene HD Transfection Reagent following the manufacturer's instructions (Roche Applied Science, Indianapolis, IN). Cells were used for electrophysiological experiments 24–48 h after transfenction.

2.3. Whole-cell patch-clamp recording

Whole-cell currents were recorded using a Patch/Whole Cell Clamp Amplifier Axopatch 200B (Axon Instruments, Foster City, CA) and A/D converter (Digidata 1200, Axon Instruments) at room temperature. Data acquisition was performed using PCLAMP7 software (Axon Instrumets). Capacitative components were electrically compensated. Leak subtraction was performed by the P/N method ($N = 4–6$).

The resistance of recording pipettes was 2–3 MΩ when filled with the pipette solution containing 120 mM $CsMeSO_4$, 20 mM tetraethylammonium chloride, 14 mM EGTA, 5 mM Mg-ATP, 5 mM Na_2 creatine phosphate, 0.2 mM GTP, and 10 mM HEPES (pH 7.3, adjusted with CsOH at room temperature). The external solution contained 137 mM NaCl, 5.4 mM KCl, 1 mM MgCl, 10 mM HEPES, 10 mM glucose, and 2 mM $BaCl_2$ (pH 7.4, adjusted with NaOH at room temperature). In our experiments, 75–95% of cells transfected with various plasmids were positive for the Ca^{2+} channel currents. The liquid junction potential, calculated to be 16.3 mV, was not corrected in this study because all of the experiments were carried out with the same pipette solution and external solution.

2.4. Preparation of cell extracts and immunoblot analysis

BHK6 cells were transfected with a plasmid bearing $Ca_v1.2$ cDNA or its mutants using Lipofectamine Plus following the manufacturer's instructions (Invitrogen). Forty-eight hours after transfection, the cells were washed with PBS, and lysed in lysis buffer (140 mM NaCl, 10 mM Tris–HCl [pH 7.4], 5 mM EDTA, 5 mM EGTA, 1% NP-40, and 3 mM pepstatin A). The protein concentration was determined by the method of Lowry et al. [14] and 40 mg of protein in SDS-sample buffer [15] was applied to an SDS-polyacrylamide gel (4–12%). The gel was then subjected to Western blotting. Detection of $Ca_v1.2$ and its mutant proteins was performed using antibodies against $Ca_v1.2$ (rabbit anti-CNC1; ACC-003, Alomone Labs, Jerusalem, Israel). The secondary antibody was anti-rabbit immunoglobulin G conjugated with horseradish peroxidase (NA934V, GE Healthcare Bio-Sciences Corp., Piscataway, NJ).

2.5. Immunofluorescence microscopy

BHK6 cells transfected with a plasmid bearing $Ca_v1.2$ cDNA or its mutants were prepared as described above. Forty-eight hours after transfection, the cells were washed with PBS, fixed with 4% formaldehyde for 10 min, permeabilized with methanol for 3 min, and blocked with PBS-T solution (3.2 mM Na_2HPO_4, 0.5 mM KH_2PO_4, 135 mM NaCl, 1.3 mM KCl, and 0.05% Tween20, pH 7.4) containing 5 mg/ml of bovine serum albumin for 30 min at room temperature. The primary antibody, anti-CNC1, was visualized with a secondary antibody labeled with Alexa Fluor498 (Invitorogen). Nuclei were labeled with Hoechst 33342 (Molecular Probes, OR, USA). Images were acquired with a laser-scanning confocal microscope (LSM-510 META, Carl Zeiss, Inc., Oberkochen, Germany).

2.6. Co-immunoprecipitation

tsA201 cells co-transfected with a plasmid bearing $Ca_v1.2$ or its mutants, either β_{1a} or β_{2c} and α_2/δ_1 subunits were prepared as described above. Forty-eight hours after transfection, to prepare cell lysates, the cells were washed with PBS, collected with a rubber policeman in TNE buffer (140 m NaCl, 10 mM Tris–HCl [pH 7.4], 5 mM EDTA-3Na, 5 mM EGTA, 1% NP-40, and 3 μM pepstatin) containing a protease inhibitor cocktail (Roche Diagnostics GmbH, Mannheim, Germany, Cat, no. 04 693 159 001) added at a ratio of one tablet of the cocktail to 10 ml of TNE buffer, and lysed by homogenization. Antibodies against $Ca_v1.2$ (rabbit anti-CNC1; ACC-003, Alomone Labs) were added to the cell lysate and the mixture was incubated with rotation for 16 h at 4 °C. Dynabeads protein G (Invitrogen Dynal, Oslo, Norway) was used to precipitate antibody–protein complexes. Co-precipitated proteins were identified by Western blotting with a primary antibody against the β subunit that detects both β_{1a} and β_{2c} subunits (mouse anti-CACNB2; H00000783-M05, Abnova Coporation, Taipei, Taiwan) and a secondary anti-mouse immunoglobulin G conjugated with horseradish peroxidase (NA9310V, GE Healthcare Bio-Sciences).

2.7. Statistical analysis

All data are presented as the mean ± SEM, and statistical significance was determined using the unpaired Student's t test with a value of $p < 0.05$ required for significance.

3. Results

3.1. Gly residues in the S2–S3 linkers of domains I and II are highly conserved

Since VGCCs contain four structurally conserved domains, we predicted that a Gly residue, which corresponds positionally to the Gly residue in the S2–S3 linker of domain III described in our previous study [11], is conserved in the S2–S3 linkers of other domains of various VGCCs from various species. A multiple amino acid sequence alignment revealed that the Gly residue was also completely conserved in the S2–S3 linker of domain I, and highly conserved in the S2–S3 linker of domain II (Fig. 1B). The relative positions of these Gly residues are shown in Fig. 1A, based on conventional membrane topology. The Gly residue in domain II of yeast VGCC homologues was found to be replaced with a hydrophobic amino acid residue, such as Leu, Phe or Ala (Fig. 1B). In addition, we found that the Gly residue in domain IV was not conserved in animal L-type VGCCs, including $Ca_v1.2$ (see below). We, therefore, focused on the Gly residues in domains I and II of $Ca_v1.2$ in this study.

3.2. Effect of substituting Glu or Gln for Gly^{182} and Gly^{579} on peak current density and the current–voltage relationship

We have shown previously that changing Gly to Glu in the domain III S2–S3 linkers of $Ca_v1.2$ and yeast Cch1 results in a complete loss of function [11]. Here, to investigate the roles of Gly^{182} and Gly^{579} in domains I and II of $Ca_v1.2$, respectively, we replaced them with Glu to produce the mutant $Ca_v1.2$, G182E and G579E. Since Glu has a negative charge and the Gly to Glu substitution may cause a drastic structural change of $Ca_v1.2$ and/or an artificial protein–protein interaction due to ionic bonding, we also replaced them with Gln that has no charge with almost the same residue volume as that of Glu. The resulting mutant $Ca_V1.2$s were named G182Q and G579Q, respectively. These mutant $Ca_v1.2$s were transfected into BHK6 cells stably expressing rabbit β and α_2/δsubunits.

We first tested the peak current density of the transfected cells using a whole-cell patch-clamp with 2 mM Ba^{2+} as a charge carrier. When the cells were depolarized from a holding potential of −80 mV to −10 mV, the peak current density of $Ca_v1.2$ used as a control was −516 pA/pF ($n=23$) (Fig. 2A). By contrast, no current was detected in some

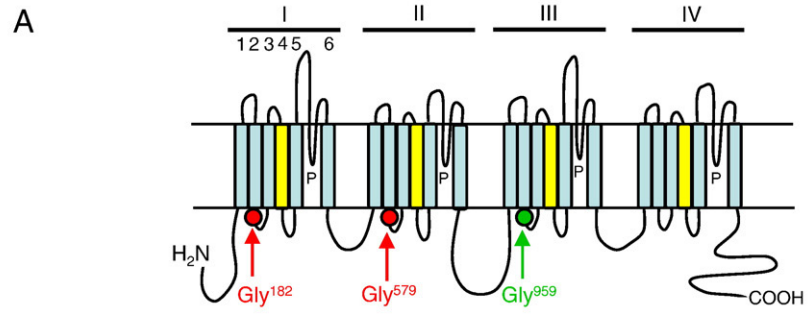

B

Species	Protein	Type	NCBI-GI No.	Domain I Sequence (S2)	Domain II Sequence (S2)
R. norvegicus	$Ca_v1.2c$(rbCII)	L	AAA18905	158-NLERVEYLFLIIFTVEAFLKVIAYGLLFHP	555-VQDTANKALLALFTAEMLLKMYSLGLQAYF
	$Ca_v1.2$ (α_{1C})	L	NP036649	188-NLERVEYLFLIIFTVEAFLKVIAYGLLFHP	585-VQDTANKALLALFTAEMLLKMYSLGLQAYF
	$Ca_v1.3$ (α_{1D})	L	NP058994	160-NLEKVEYAFLIIFTVETFLKIIASGLLLHP	613-IQDIANKVLLALFTCEMLVKMYSLGLQAYF
	$Ca_v1.4$ (α_{1F})	L	NP446153	126-NLEQVEYVFLVIFTVKTVLKIVAYGLVLHP	560-TQEYANKVLLCLFTVEMLLKLYGLGPSVYV
	$Ca_v2.1$ (α_{1A})	P/Q	NP037050	134-RLDDTEPYFIGIFCFEAGIKIVALGFAFHK	520-FLYYAEFIFLGLFMSEMFIKMYGLGTRPYF
	$Ca_v2.2$ (α_{1B})	N	NP671482	129-RLDDTEPYFIGIFCFEAGIKIIALGFVFHK	513-ALYFAEFVFLGLFLTEMSLKMYGLGPRSYF
	$Ca_v2.3$ (α_{1E})	R	NP062167	74-RLEKTEPYFIGIFCFEAGIKIVALGFIFHK	458-LLYYAEFLFLGLFLLEMSLKMYGMGPRLYF
	$Ca_v3.1$ (α_{1G})	T	NP113789	116-ILQAFDDFIFAFFAVEMVVKMVALGIFGKK	775-ALEISNIVFTSLFALEMLLKLLVYGPFGYI
	$Ca_v3.2$ (α_{1H})	T	AAG35187	135-ILEAFDDFIFAFFAVEMVIKMVALGLFGQK	821-ALEISNIVFTSMFALEMLLKLLACGPLGYI
	$Ca_v3.3$ (α_{1I})	T	NP064469	112-ILQVFDDFIFIFFAMEMVLKMVALGIFGKK	629-ILEICNVVFTSMFALEMILKLAAFGLFDYL
	VGCNL1(Rb21)	?	NP705894	70-VTFTLDTLLMFLYTAEMIAKMHIRGIVKGD	417-EFYLAEVAFTVLFDLEALLKIWCLGFTGYI
H. roretzi	TuCa1	L	BAA34927.2	81-ILEKVEYIFLGIFTIEAILKIIAYGLFFHP	460-AQDLANKILLTLFTIEMLVKMYSLGMQQYF
C. capillata	VGCCα_1	L	AAC63050.1	147-DLEVAEYFFLAVFAIEGLLKIIAYGFILHP	528-FLDRANYFFLGLFTFEMLLKIYCLGIYGYL
S. pombe	VIC	?	NP593894	215-TIDYLIIVIGILYTLEMLLKIYLFGFLYDG	547-RYLIFYACVDFLLAAEVILRFFAYLPDYRL
C. albicans	Cch1	?	AAN86029	453-WADYLLMVINVIYTAEVIGKIIAYGFYDDH	936-LLYRFEASFTGVFMVEIILRFAFYFPNWRL
A. gossypi	Cch1	?	NP983261	308-WSDSAFILCNCLFTAEMFAKIIAFGFWDDS	722-LAYKFERILSFVLMIETLIRLFLYAPAFWK
S. cerevisiae	Cch1	?	NP011733	380-WTDYFIFILSACFTGNDIAKIIAFGFWDDS	801-ILLKTDRGISIVLFIESLARLVLYLPNMWK
	Consensus sequence			.....E..F...F..E...K....G..... (*)	.....E..F...F..E...K....G.....
				D I Y R	N L L R
				L H	D I

Fig. 1. Highly conserved Gly residues. (A) Location of the highly conserved Gly residues in the S2–S3 linkers of VGCC α_1 subunits. The Gly residues highly conserved in the S2–S3 linkers of domains I–III of VGCC α_1 subunits are shown with red circles (analyzed in this study) and a green circle (analyzed in our previous study [11]). The Roman numerals I–IV represent four homologous domains and the Arabic numerals 1–6 represent putative transmembrane segments (S1–S6). P represents the putative pore loop. The putative S4 segments in domains I–IV, containing repeated motifs of a positively charged residue followed by two hydrophobic residues, are colored yellow. The N- and C-termini are located in the cytoplasm. (B) Multiple amino acid sequence alignment of the S2–S3 linkers of domains I and II of various VGCC α_1 subunits and candidates. Multiple amino acid sequence alignment was performed with ClustalW (http://align.genome.jp/). Highly conserved Gly residues are colored red. The putative transmembrane segments S2 and S3 were predicted based on Jan and Jan [48] and underlined. The full names of the species are (from top to bottom): *Rattus norvegicus*; *Halocynthia roretzi*; *Cyanea capillata*; *Schizosaccharomyces pombe*; *Candida albicans*; *Ashbya gossypii*; and *Saccharomyces cerevisiae*.

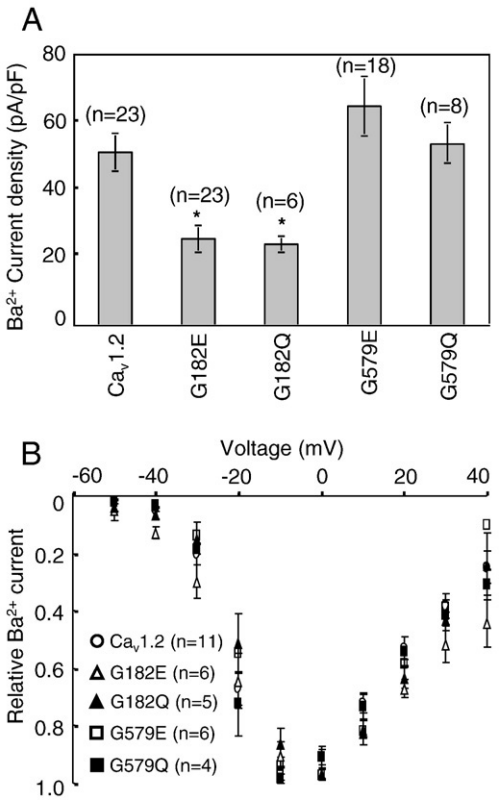

Fig. 2. Effect of substituting Glu or Gln for Gly^{182} and Gly^{579} on current density and current–voltage relationships. (A) Peak current density of BHK6 cells expressing $Ca_v1.2$ or its mutants. Whole-cell currents were recorded with 100 ms depolarization to −10 mV from a holding potential of −80 mV with 2 mM Ba^{2+}. (B) Current–voltage relationships for the channels of $Ca_v1.2$ (open circle), G182E (open triangle), G182Q (closed triangle), G579E (open square), and G579Q (closed square). Error bars represent the mean ± S.E.M. The number of BHK6 cells tested is indicated in parentheses. *, $p<0.001$ vs. $Ca_v1.2$ (control).

populations of cells expressing G182E or G182Q, and the peak current density of detectable cells was −25 ± 4 pA/pF ($n=23$) for G182E and −24 ± 2 pA/pF ($n=8$) for G182Q, each significantly smaller than that of $Ca_v1.2$ ($p<0.001$). G182Q channel currents were observed in approximately 75% of the patch-clamped cells, whereas in wild-type $Ca_v1.2$, the currents were recorded in about 95% of the cells. On the other hand, no significant difference in peak current density between the Gly^{579} mutants (G579E, −64 ± 9 pA/pF [$n=18$]; G579Q, −53 ± 6 pA/pF [$n=8$]) and $Ca_v1.2$ was observed (Fig. 2A). These results demonstrate that the substitution of Glu or Gln for Gly^{182} decreases the peak current density of $Ca_v1.2$ and that this decrease is independent of the charge of the substituted amino acid.

To examine whether the substitution of Gly^{182} or Gly^{579} with Glu or Gln alters the voltage-dependence of current activation, we investigated the current–voltage (I–V) relationships. As shown in Fig. 2B, $Ca_v1.2$ and its mutants showed a maximum current at approximately −10 mV and the I–V relationship of $Ca_v1.2$ was not significantly changed by the G182E, G182Q, G579E and G579Q mutations. These results indicate that the Gly to Glu or Gln substitution in the S2–S3 linker of domains I and II does not perturb the voltage-sensing and activation properties of $Ca_v1.2$.

3.3. Effect of substituting Glu or Gln for Gly^{182} or Gly^{579} on the stability and localization of the mutant proteins

To search for the cause of the loss or decrease of peak current density produced by the amino acid substitutions described above, we examined the stability and subcellular localization of the G182E and G182Q mutant proteins. Western blot analysis showed that the amounts of G182E and G182Q were essentially the same as the amount of $Ca_v1.2$ (Fig. 3A). Using immunofluorescence microscopy with an antibody specific to the II–III loop of $Ca_v1.2$, we observed that the $Ca_v1.2$ proteins were localized to the plasma membrane (Fig. 3B, panel a). However, the majority of the G182E and G182Q proteins appeared to be present in the cytoplasm (Fig. 3B, panels b and c). These results indicate that the substitution of Glu or Gln for Gly^{182} did not affect the expression of the mutant proteins, but resulted in their mislocalization. Thus, it is likely that the absence of current or low peak current density of cells expressing G182E or G182Q is due to the mislocalization of these mutant proteins.

Several reports have indicated that the auxiliary β subunit plays a crucial role in membrane trafficking of the α_1 subunit [7,16]. It is possible that the G182E and G182Q mutations impaired the interaction between α_1 and β subunits, thus leading to the mislocalization of α_1 subunit. To examine this possibility, we performed immunoprecipitation experiments with antibodies against $Ca_v1.2$. We found that the Gl82E and G182Q proteins were co-immunoprecipitated with the β subunit, such as β_{1a} and β_{2c} subunit, and that the level of the precipitated β subunit was comparable between the mutant proteins and $Ca_v1.2$ on the immunoblots. Fig. 4 shows that the amount of the β subunit immunoprecipitated with the G182E or G182Q protein was essentially the same as that immunoprecipitated with $Ca_v1.2$, suggesting that the G182E and G182Q mutations do not affect the interaction between the α_1 and β subunits.

We also examined effects of the G579E and G579Q mutations on the expression and localization of the corresponding mutant proteins. As shown in Fig. 3A, the amounts of the G579E and G579Q proteins were the same as the amount of $Ca_v1.2$. The immunofluorescence microscopy showed that the G579E proteins were localized to the plasma membrane, like $Ca_v1.2$ (Fig. 3B, panel d). On the other hand, although a certain amount of G579Q was observed in the cytoplasm, the majority of this protein was localized to the plasma membrane (Fig. 3B, panel e). These results indicate that the substitution of Gly^{579} with Glu or Gln had no serious effect on the expression and localization of $Ca_v1.2$.

3.4. Effect of substituting Glu or Gln for Gly^{182} or Gly^{579} on the voltage-dependent inactivation

To study whether the substitution of Glu or Gln for Gly^{182} or Gly^{579} produces any other effect on the electrophysiological properties of $Ca_v1.2$, we analyzed VDI kinetics of cells expressing these substituted proteins. VDI profiles of $Ca_v1.2$ and its mutants were resolved by a 2000 ms-depolarization step from a holding potential of −80 mV to −10 mV in the presence of 2 mM Ba^{2+} as a charge carrier (Fig. 5A–D). Components and time constants of VDI kinetics were analyzed by fitting the current trance with double exponential functions (Fig. 5E and F). As for G579E, its constant component relative to the total current was comparable to that of $Ca_v1.2$ (Fig. 5E). However, its fast component was half as large as that of $Ca_v1.2$ and the slow component was 1.7-fold larger than that of $Ca_v1.2$ (Fig. 5E). In addition, the fast and slow time constants were 113 ± 6 ms and 628 ± 43 ms ($n=6$) for $Ca_v1.2$, whereas they were 170 ± 16 ms and 978 ± 55 ms ($n=6$) for G579E, respectively (Fig. 5F and G). These results indicate that the G579E mutation slows the VDI kinetics of $Ca_v1.2$. In contrast to G579E, the effects of the G579Q mutation were mild. The fast and slow inactivation components were 0.7-fold smaller and 1.4-fold larger than those of $Ca_v1.2$, respectively (Fig. 5E), and its fast and slow time constants (99 ± 9 ms and 603 ± 39 ms, respectively) were essentially the same as those of $Ca_v1.2$ (Fig. 5F and G). These results suggest that the effect of the Gly^{579} to Glu substitution on VDI is brought about principally by the negative charge of the substituted Glu.

Since the G182E and G182Q mutations had essentially the same effect on peak current density and protein localization, we only analyzed the VDI kinetics of the G182E mutant. The fast and slow

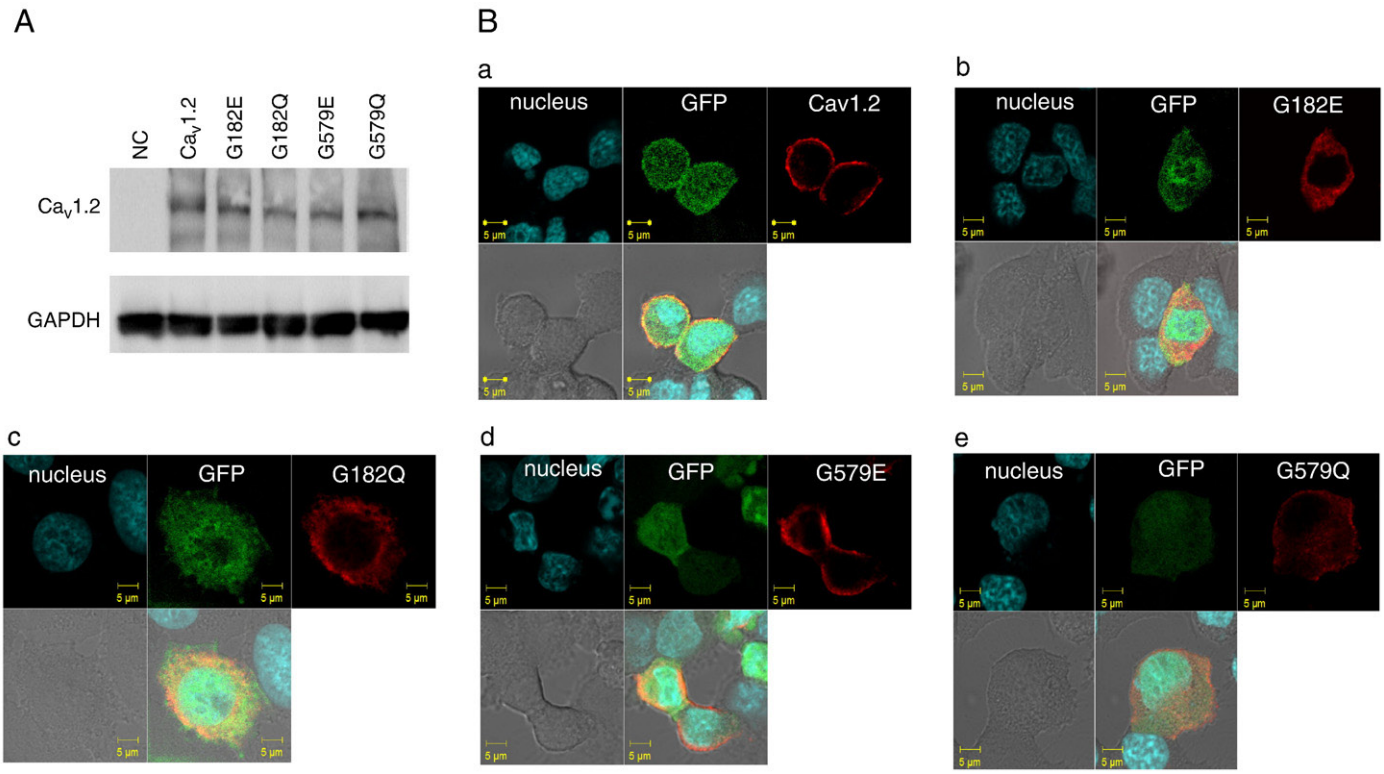

Fig. 3. Effect of substituting Glu or Gln for Gly^{182} and Gly^{579} on the expression and localization of the mutant proteins. (A) Expression of $Ca_v1.2$ and its mutant proteins. BHK6 cells were transfected with the same amount of a plasmid bearing $Ca_v1.2$, G182E, G182Q, G579E, or G579Q cDNA. NC represents non-transfected cells as a negative control. Total cell extract (40 μg) was subjected to an immunoblot analysis with antibodies to $Ca_v1.2$ and GAPDH (glyceraldehyde-3-phosphate dehydrogenase), an internal control protein used for examining the amount of protein applied. (B) Subcellular localization of $Ca_v1.2$ and its mutants. BHK6 cells were observed by confocal laser-scanning microscopy 48 h after transfection with the same amount of plasmid bearing the following cDNA: $Ca_v1.2$ (a), G182E (b), G182Q (c), G579E (d), and G579Q (e). blue, nuclear staining with Hoechst 33342; green, GFP; red, $Ca_v1.2$ and its mutants detected with antibodies to $Ca_v1.2$.

components of G182E were not significantly different from those of $Ca_v1.2$ (Fig. 5E), but the time constants of the fast and slow components of G182E (887 ± 63 ms and 152 ± 9 ms, respectively) were significantly larger than those of $Ca_v1.2$ (Fig. 5F).

3.5. Effect of the G579E mutation on steady-state inactivation

We assessed the steady-state voltage-dependence of current inactivation of G579E in 2 mM Ba^{2+}. The whole-cell currents were recorded at −10 mV after a series of 5-s-conditioning pre-pulses applied between −90 and +10 mV. Compared to $Ca_v1.2$, no shift of the voltage-dependence of the steady-state inactivation curve was observed in G579E (Fig. 6).

Since currents through the G182E and G182Q channels were small and cells expressing the channels were faltering, we could not estimate successfully their steady-state inactivation curves.

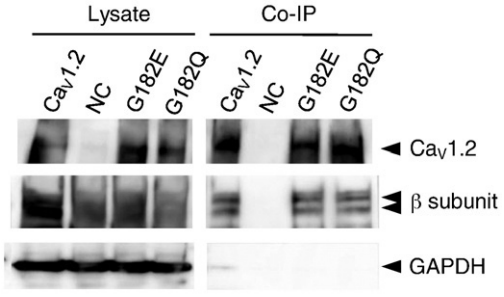

Fig. 4. Co-immunoprecipitation of G182E and G182Q with β_{2c} subunit. The same amount of a plasmid carrying cDNA encoding $Ca_v1.2$, G182E, or G182Q was co-transfected with that coding for β_{2c} and α_2/δ subunits into tsA201 cells. Antibodies against $Ca_v1.2$ were added to cell lysates and after a 16-h incubation, antibody–protein complexes were precipitated with Dynabeads protein G. Co-precipitated proteins were identified by Western blotting with primary antibodies against α subunit, β subunit or glyceraldehyde-3-phosphate dehydrogenase (GAPDH). The negative control (NC) represents cells transfected with an empty vector for $Ca_v1.2$ cDNA. Co-IP, co-immunoprecipitated samples.

4. Discussion

In this study, we have focused on two highly conserved Gly residues of the VGCC α_1 subunit $Ca_v1.2$: one is Gly^{182} located in the S2–S3 linker of domain I and the other, Gly^{579} in the S2–S3 linker of domain II (Fig. 1). The reason for this focus is that the two Gly residues have been highly conserved during evolution and correspond positionally to Gly^{959} in the S2–S3 linker of domain III. Our previous study has shown that the Gly^{959} residue is completely conserved from yeasts to humans and essential for channel activity [11]. We, therefore, addressed a question as to what are the roles of Gly^{182} and Gly^{579} in the functional regulation of $Ca_v1.2$.

4.1. Role of Gly^{182}

Our studies have shown that the current–voltage relationships of the G182E and G182Q mutants are similar to those of $Ca_v1.2$. However, G182E and G182Q have little or no current density compared to $Ca_v1.2$ (Fig. 2). This phenotype is not due to a loss of protein expression because the amount of each mutant in cells was essentially the same as that of $Ca_v1.2$ (Fig. 3A). However, immunofluorescence microscopy has shown that the majority of the G182E and G182Q proteins seem to be present in the cytoplasm (Fig. 3B). Thus, the small current density of G182E and G182Q suggests that only a limited amount of the mutant proteins, which can be hardly detected by fluorescence microscopy, is localized to

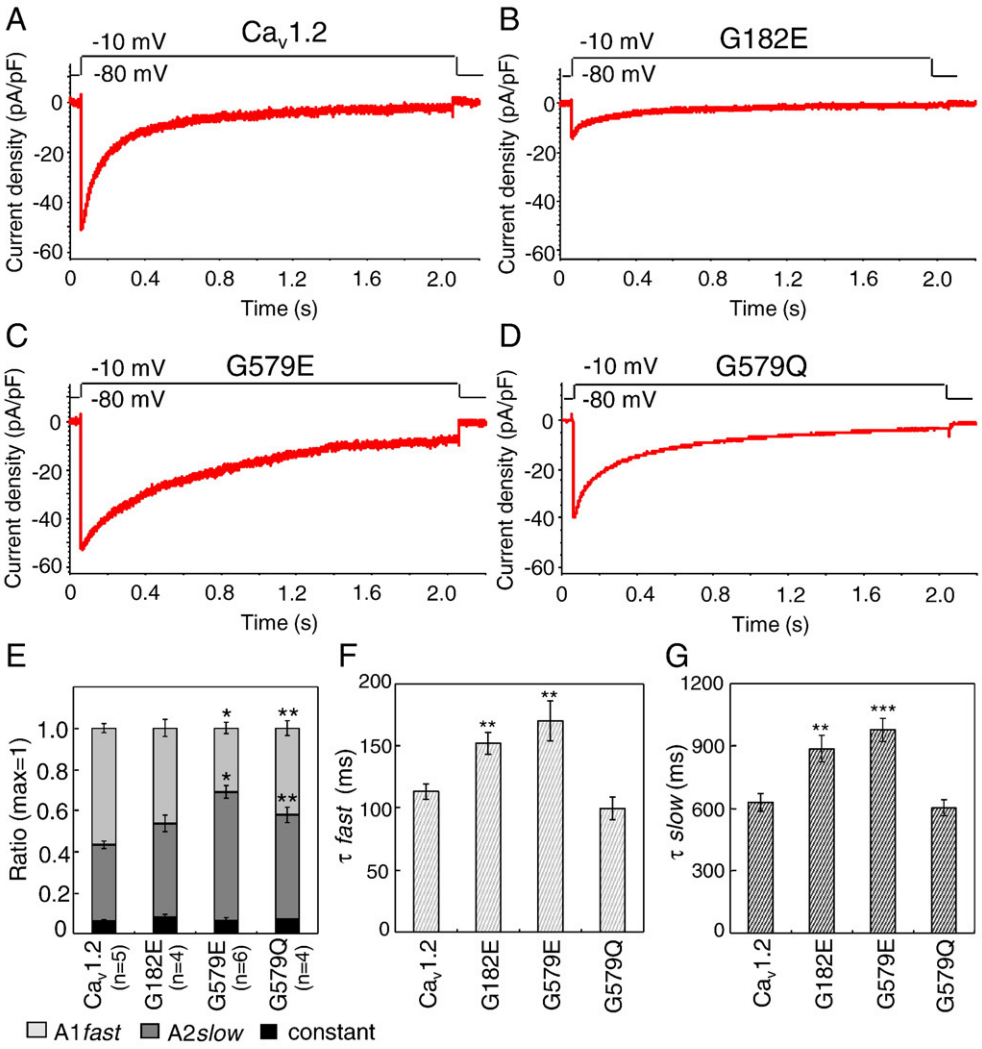

Fig. 5. Effect of substituting Glu or Gln for Gly^{182} and Gly^{579} on VDI. Currents were elicited by applying step depolarizations to −10 mV for 2000 ms from a holding potential of −80 mV in BHK6 cells expressing $Ca_v1.2$ or its mutants with 2 mM Ba^{2+} as a charge carrier. (A) $Ca_v1.2$; (B) G579E; (C) G579Q; (D) G182E. Components and time constants of VDI were analyzed by fitting the current trance with double exponential functions, $I(t) = A1_{fast} \times \exp(-t/t_{fast}) + A2_{slow} \times \exp(-t/t_{slow}) + \text{constant}$. (E) Comparison of components; (F) comparison of t_{fast}; (G) comparison of t_{slow}. Error bars represent the mean ± S.E.M. The number of BHK6 cells tested is indicated in parentheses. *, $p<0.0001$; **, $p<0.05$; ***, $p<0.001$ (vs. $Ca_v1.2$).

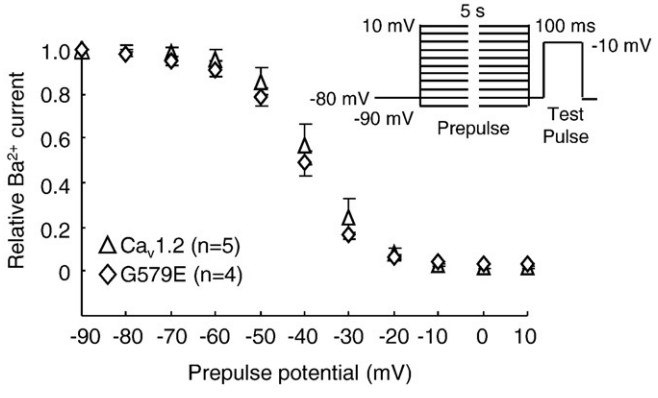

Fig. 6. Effect of the G579E mutation on steady-state inactivation. The voltage-dependence of availability of each Ca^{2+} channels are expressed as relative amplitude of Ba^{2+} currents through $Ca_v1.2$ (triangle) and G579E (diamond). The protocol is shown in the inset. Ba^{2+} currents were measured with a test pulse to −10 mV following a 5-s-conditioning pre-pulse to between −90 and 10 mV. The interval between each episode was 60-s. Error bars represent the mean ± S.E.M. The number of BHK6 cells tested is indicated in parentheses.

the plasma membrane and then becomes partially functional. The charge of the substituted amino acid (Glu) is not the cause of the mislocalization and small current density because the G182E and G182Q mutants exhibit essentially the same phenotype. Alternatively, a large residue volume of the substituted Glu or Gln could be a major cause of these phenotypes. It is suggested that the Gly^{959} residue in the domain III S2–S3 linker is important for a spatial arrangement of the S2–S3 segments [11]. Likewise, the Gly^{182} residue of domain I may be important for the spatial arrangement of the S2–S3 segment and this spatial rearrangement could be important for a proper surface expression of $Ca_v1.2$.

Surface expression of the L-type VGCC α_1 subunit is regulated by several factors. It is known that β subunits bind to the AID on the I–II linker region of α_1 subunits in the endoplasmic reticulum (ER) and thus promotes the translocation of α_1 subunits to the plasma membrane [7,16]. α_2/δ subunits appear to interact with an extracellular loop of α_1 subunits in the ER to transfer it to the cell surface and stabilize its expression in the plasma membrane [17,18]. The RGK family of small G proteins alters trafficking of α_1 subunits to the plasma membrane via the interaction with β subunits [19–21]. Our immunoprecipitation experiments in vitro have suggested that the G182E and G182Q mutations do not abolish the interaction between α_1 and β subunits (Fig. 4). Thus, it is likely that any structural change

caused by the G182E and G182Q mutations does not affect the interaction between α_1 and β subunits in vivo but may alter other factors involved in the membrane trafficking of VGCCs and/or the maintenance of their surface expression. Several such factors have been reported. For example, the postsynaptic scaffolding protein AKAP79 mediates trafficking of α_1 subunits [22]. Recent studies have shown that PEST-mediated protein degradation plays a crucial role in the regulation of the stability of the surface expression of VGCC [3,23]. Further study is necessary to elucidate a possible role of the Gly^{182} residue in the membrane trafficking of $Ca_v1.2$.

4.2. Role of Gly^{579}

We have also shown that substitution of Gly^{579} with Glu or Gln produces no obvious change in the expression, subcellular localization, or current density of the mutant proteins G579E and G579Q (Figs. 2 and 3). However, the substitution of Gly^{579} with a negatively charged Glu (G579E) slowed VDI without affecting steady-state inactivation, and this effect on VDI was not seen when an uncharged Gln was substituted for Gly^{579} (G579Q) (Fig. 5). These results indicate that Gly^{579} bears an important role for the regulation of the voltage-dependent inactivation of the L-type Ca^{2+} channel.

The inactivation of channels provides a negative feedback loop to control the degree of Ca^{2+} influx and prevents overloading of the cell with Ca^{2+}. In L-type VGCCs, two processes inactivate Ca^{2+} currents: Ca^{2+}-dependent inactivation (CDI) and VDI [24,25]. Several studies have suggested that CDI and VDI are mediated by common components [26,27]. The two processes can be separated by replacing extracellular Ca^{2+} with Ba^{2+}. It is well established that the linker of domains I and II of α_1 subunits interacts with β subunits and is essential for VDI [4,25–27]. In addition, multiple regions within α_1 subunits, including pore-forming transmembrane segments [28,29], the I–II and II–III linkers [10,30–32] and the C-terminal region [31,33], have been shown to be involved in VDI. Several hypotheses have been proposed for the importance of the structural change of multiple regions of α_1 subunits upon VDI. One is that the binding of β subunits to the AID of α_1 subunits located in the I–II intracellular loop slows VDI by restricting the movement of the IS6 segment [34]. Also, it is proposed that the distortion of the putative 'teepee' structure of pore-forming S5 and S6 segments is important for gating inactivation [35]. Mutations in the pore-forming segments S5 and S6 may alter the 'teepee' structure, thereby impairing the transition between opening and inactivation of the channel. Further, the domain linkers and the C-terminal region may form part of separate inactivation gates and mediate the inactivation via the occlusion of the inner channel mouth [10,35]. Here we have shown that the mutation of Gly^{579} in the S2–S3 linker of domain II alters VDI gating, depending upon the charge of the substituted amino acid. It is possible that the introduction of a negatively charged amino acid residue impedes the conformational change required or VDI.

In the present study, we did not analyze the reversal potential of Ca^{2+} channel currents because depolarization to potentials higher than +40 mV activates endogenous outward currents that are also sensitive to Cd^{2+} in BHK6 cells. Therefore, the effect of mutations on the ion selectivity of the Ca^{2+} channel is to be studied in future experiments.

4.3. Importance of Gly and Pro in the S2–S3 linker of ion channels

The present study on $Ca_v1.2$ shows the potential importance of the VGCC S2–S3 linker that has received less attention than other linkers.

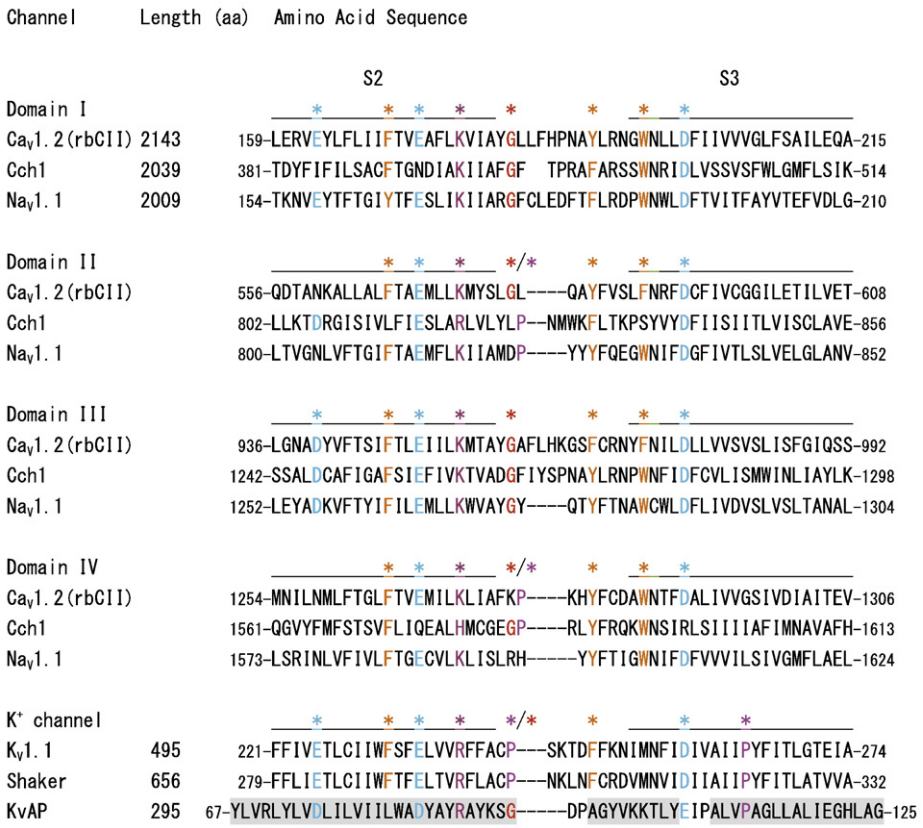

Fig. 7. Multiple amino acid sequence alignment of the S2-linker-S3 regions of voltage-gated Ca^{2+}, Na^+, and K^+ channels and a yeast Ca^{2+} channel homolog. Highly conserved Gly and Pro residues, which are two or three amino acids downstream from the S2 segment, are colored red and pink, respectively. Other highly conserved amino acids are also colored other colors. The putative transmembrane segments S2 and S3 of various ion channels except for KvAP were predicted based on Jan and Jan [48] and upperlined. The putative transmembrane segments S2, S3A, and S3B of KvAP were based on the X-ray structure [36] and hatched. Accession numbers of the channels listed here are as follows. $Ca_v1.2$ (rbCII), AAA18905; Cch1, NP_011733; $Na_v1.1$, NP_110502; Kv1.1, NP_775118; Shaker, CAA29917; KvAP, NP_147625.

The G–E and G–Q mutations in the domain I S2–S3 linker resulted in the mislocalization of $Ca_v1.2$, leading to a small current density (Figs. 2 and 3) and the G–E mutation in the domain II S2–S3 linker brought about a slow DVI (Fig. 5). In addition, our previous study has shown that the G–E mutation in the domain III S2–S3 linker causes a loss-of-function of $Ca_v1.2$ [11].

To explore the significance of the Gly residues of the S2–S3 linker, we aligned the amino acid sequences of the S2-linker-S3 regions of various VGCCs and structurally related Na^+ and K^+ channel (Fig. 7 and Supplementary Figs. 1–4). Based on this alignment, it is evident that Gly is completely conserved in the S2–S3 linkers of domains I, II, and III of VGCCs that we searched. However, in L-type VGCCs, Gly is not completely conserved in the S2–S3 linker of domains IV. It is noteworthy that there is a rule: if Gly is absent, Pro is present at the next position.

In voltage-gated Na^+ channels, Gly is also completely conserved in the S2–S3 linkers of domains I and III (Fig. 7). Interestingly, the above rule is applicable to the S2–S3 linker of domain II, where Pro is present instead of Gly at the next position. Neither Gly nor Pro is present in the S2–S3 linker of domain IV.

As for voltage-gated K^+ channels, including Shaker, Pro is highly conserved instead of Gly in the S2–S3 linker of the most of the K^+ channels we searched. The KCNQ family of the K^+ channels has Gly at the position corresponding to that of Gly in VGCCs, while the KCNH family has Pro at a different position between the putative S2 and S3 segments.

What is the importance of the Gly or Pro residue in the S2–S3 linker? X-ray structure of KvAP voltage-gated K^+ channel has indicated that the conserved Gly is located in the turn connecting the S2 and S3 segments [36]. As mentioned above, in most of other voltage-gated K^+ channels, including Shaker, this Gly corresponds to the Pro residue, confirming the importance of a turn at this position. Therefore, it is likely that the effect of the mutations that we made at this position is to disrupt the tertiary structure of the voltage sensor paddle, leading to the alteration of kinetics and functional expression of $Ca_v1.2$. This idea is supported by studies in Shaker, where disruption of the paddle alters surface expression [37].

There are a few examples showing the physiological relevance of the S2–S3 linkers. In the $Ca_v3.2$ T-type VGCC, the Phe-Leu mutation in the domain I S2–S3 linker results in an approximately 10 mV hyperpolarizing shift in the half-activation potential without affecting gating, thus mediating a gain-of-function effect on this channel [38,39]. This mutation is associated with childhood absence epilepsy [40]. It was also reported that the A–D mutation in the domain III S2–S3 linker of $Ca_v1.4$ appears to exert no detectable changes in the activation, inactivation, or conductance properties of the channel, but is associated with incomplete X-lined congenital stationary night blindness [41]. The authors of this report speculate that channel activity in intact photoreceptors is very tightly regulated and thus photoreceptor synaptic transmission becomes defective due to subtle, yet undetectable, changes in channel activity.

Although examples indicative of the importance of the VGCC S2–S3 linkers are limited, a considerable number of examples have been reported for the S2–S3 linker of voltage-gated K^+ channels [42–47]. These include a deficiency of surface expression and a change of the gating kinetics of VGKCs. The above examples for VGCCs and voltage-gated K^+ channels suggest that the S2–S3 linkers have crucial roles in the function and membrane trafficking of the channels.

In summary, our present and previous studies have shown that the three Gly residues conserved in the S2–S3 linkers of domains I, II, and III have different essential roles for channel function. These findings should provide clues to a deeper understanding of the structure–function relationship of VGCCs.

Acknowledgements

We express our sincere thanks to Prof. Terrance P. Snutch (University of British Columbia) for generous gift of rat brain $Ca_V1.2$ (rbCII), Prof. Yasuo Mori (Kyoto University) for BHK6 cells, Prof. Hiromichi Tsuru (Toho University, Tokyo) for encouragement, Prof. Yoshihiro Kubo (National Institute for Physiological Sciences, Okazaki) for discussion, reviewers of this paper for valuable comments, and Ms. Yumiko Higashi (Tokyo Gakugei University) for her secretarial work. This work was supported by Grants-in-Aid for Scientific Research on Priority Areas (no. 21026009 to H.I, and no. 20056029 to S.A-A.), a Grant-in-Aid for Scientific Research B (no. 21370017 to H.I.), a Grant-in-Aid for Scientific Research C (no. 20570158 to K.I.), a grant of strategic basis on research grounds for non-governmental schools (no. 13809 to S.A-A.) from the Ministry of Education, Culture, Sports, Science and Technology in Japan, a grant from The Novartis Foundation (Japan) for the Promotion of Science (no. KEN20-191 to H.I.), and a grant for the Frontiers of Membrane Protein Research (the Joint Project between Institute for Protein Research, Osaka University and Okazaki Institute for Integrative Bioscience (to H.I.).

Appendix A. Supplementary data

Supplementary data associated with this article can be found, in the online version, at doi:10.1016/j.bbamem.2010.01.004.

References

[1] M.J. Berridge, M.D. Bootman, H.L. Roderick, Calcium signalling: dynamics, homeostasis and remodeling, Nat. Rev. Mol. Cell. Biol. 4 (2003) 517–529.
[2] W.A. Catterall, E. Perez-Reyes, T.P. Snutch, J. Striessnig, International Union of Pharmacology. XLVIII. Nomenclature and structure–function relationships of voltage-gated calcium channels, Pharmacol. Rev. 57 (2005) 411–425.
[3] S.E. Jarvis, G.W. Zamponi, Trafficking and regulation of neuronal voltage-gated calcium channels, Curr. Opin. Cell. Biol. 19 (2007) 474–482.
[4] M. Pragnell, M. De Waard, Y. Mori, T. Tanabe, T.P. Snutch, K.P. Campbell, Calcium channel β-subunit binds to a conserved motif in the I–II cytoplasmic linker of the α_1-subunit, Nature 368 (1994) 15–16.
[5] M.W. Richards, A.J. Butcher, A.C. Dolphin, Ca^{2+} channel β-subunits: structural insights AID our understanding, Trends. Pharmacol. Sci. 25 (2004) 626–632.
[6] Y.H. Chen, M.H. Li, Y. Zhang, L.L. He, Y. Yamada, A. Fitzmaurice, Y. Shen, H. Zhang, L. Tong, J. Yang, Structural basis of the α_I–β subunit interaction of voltage-gated Ca^{2+} channels, Nature 429 (2004) 675–680.
[7] D. Bichet, V. Cornet, S. Geib, E. Carlier, S. Volsen, T. Hoshi, Y. Mori, M. De Waard, The I–II loop of the Ca^{2+} channel α_1 subunit contains an endoplasmic reticulum retention signal antagonized by the β subunit, Neuron 25 (2000) 177–190.
[8] P. Pate, J. Mochca-Morales, Y. Wu, J.Z. Zhang, G.G. Rodney, I.I. Serysheva, B.Y. Williams, M.E. Anderson, S.L. Hamilton, Determinants for calmodulin binding on voltage-dependent Ca^{2+} channels, J. Biol. Chem. 275 (2000) 39786–39792.
[9] E. Kobrinsky, S. Tiwari, V.A. Maltsev, J.B. Harry, E. Lakatta, D.R. Abernethy, N.M. Soldatov, Differential role of the α_{1C} subunit tails in regulation of the $Ca_v1.2$ channel by membrane potential, β subunits, and Ca^{2+} ions, J. Biol. Chem. 280 (2005) 12474–12485.
[10] A. Livneh, R. Cohen, D. Atlas, A novel molecular inactivation determinant of voltage-gated $Ca_V1.2$ L-type Ca^{2+} channel, Neuroscience 139 (2006) 1275–1287.
[11] K. Iida, J. Teng, T. Tada, A. Saka, M. Tamai, H. Izumi-Nakaseko, S. Adachi-Akahane, H. Iida, Essential, completely conserved glycine residue in the domain III S2–S3 linker of voltage-gated calcium channel α_1 subunits in yeast and mammals, J. Biol. Chem. 282 (2007) 25659–25667.
[12] M. Wakamori, K. Yamazaki, H. Matsunodaira, T. Teramoto, I. Tanaka, T. Niidome, K. Sawada, Y. Nishizawa, N. Sekiguchi, E. Mori, Y. Mori, K. Imoto, Single tottering mutations responsible for the neuropathic phenotype of the P-type calcium channel, J. Biol. Chem. 273 (1998) 34857–34867.
[13] S. Yamaguchi, Y. Okamura, T. Nagao, S. Adachi-Akahane, Serine residue in the IIIS5-S6 linker of the L-type Ca^{2+} channel α_{1C} subunit is the critical determinant of the action of dihydropyridine Ca^{2+} channel agonists, J. Biol. Chem. 275 (2000) 41504–41511.
[14] O.H. Lowry, N.J. Rosebrough, A.L. Farr, R.J. Randall, Protein measurement with the Folin phenol reagent, J. Biol. Chem. 193 (1951) 265–275.
[15] U.K. Laemmli, Cleavage of structural proteins during the assembly of the head of bacteriophage T4, Nature 227 (1970) 680–685.
[16] T. Gao, A.J. Chien, M.M. Hosey, Complexes of the α_{1C} and β subunits generate the necessary signal for membrane targeting of class C L-type calcium channels J, Biol. Chem. 274 (1999) 2137–2144.
[17] C. Cantí, M. Nieto-Rostro, I. Foucault, F. Heblich, J. Wratten, M.W. Richards, J. Hendrich, L. Douglas, K.M. Page, A. Davies, A.C. Dolphin, The metal-ion-dependent adhesion site in the Von Willebrand factor-A domain of $\alpha_2\delta$ subunits is key to trafficking voltage-gated Ca^{2+} channels, Proc. Natl. Acad. Sci. U. S. A. 102 (2005) 11230–11235.
[18] E. Shistik, T. Ivanina, T. Puri, M. Hosey, N. Dascal, Ca^{2+} current enhancement by α_2/δ and β subunits in Xenopus oocytes: contribution of changes in channel gating and a_1 protein level, J. Physiol. 489 (1995) 55–62.

[19] P. Béguin, K. Nagashima, T. Gonoi, T. Shibasaki, K. Takahashi, Y. Kashima, N. Ozaki, K. Geering, T. Iwanaga, S. Seino, Regulation of Ca^{2+} channel expression at the cell surface by the small G-protein kir/Gem, Nature 411 (2001) 701–706.
[20] B.S. Finlin, S.M. Crump, J. Satin, D.A. Andres, Regulation of voltage-gated calcium channel activity by the Rem and Rad GTPases, Proc. Natl. Acad. Sci. U. S. A. 100 (2003) 14469–14474.
[21] P. Béguin, R.N. Mahalakshmi, K. Nagashima, D.H. Cher, N. Kuwamura, Y. Yamada, Y. Seino, W. Hunziker, Roles of 14-3-3 and calmodulin binding in subcellular localization and function of the small G-protein Rem2, Biochem. J. 390 (2005) 67–75.
[22] C. Altier, S.J. Dubel, C. Barrère, S.E. Jarvis, S.C. Stotz, R.L. Spaetgens, J.D. Scott, V. Cornet, M. De Waard, G.W. Zamponi, J. Nargeot, E. Bourinet, Trafficking of L-type calcium channels mediated by the postsynaptic scaffolding protein AKAP79, J. Biol. Chem. 277 (2002) 33598–33603.
[23] D. Catalucci, D.-H. Zhang, J. DeSantiago, F. Aimond, G. Barbara, J. Chemin, D. Bonci, E. Picht, F. Rusconi, N.D. Dalton, K.L. Peterson, S. Richard, D.M. Bers, J.H. Brown, G. Condorelli, Akt regulates L-type Ca^{2+} channel activity by modulating $Ca_v\alpha1$ protein stability, J. Cell Biol. 184 (2009) 923–933.
[24] T. Budde, S. Meuth, H.C. Pape, Calcium-dependent inactivation of neuronal calcium channels, Nat. Rev. Neurosci. 3 (2002) 873–883.
[25] T. Cens, M. Rousset, J.P. Leyris, P. Fesquet, P. Charnet, Voltage- and calcium-dependent inactivation in high voltage-gated Ca^{2+} channels, Prog. Biophys. Mol. Biol. 90 (2006) 104–117.
[26] T. Cens, S. Restituito, S. Galas, P. Charnet, Voltage and calcium use the same molecular determinants to inactivate calcium channels, J. Biol. Chem. 274 (1999) 5483–5490.
[27] I. Findlay, Physiological modulation of inactivation in L-type Ca^{2+} channels: one switch, J. Physiol. 554 (2004) 275–283.
[28] S. Hering, S. Aczél, R.L. Kraus, S. Berjukow, J. Striessnig, E.N. Timin, Molecular mechanism of use-dependent calcium channel block by phenylalkylamines: role of inactivation, Proc. Natl. Acad. Sci. U. S. A. 94 (1997) 13323–13328.
[29] C. Shi, N.M. Soldatov, Molecular determinants of voltage-dependent slow inactivation of the Ca^{2+} channel, J. Biol. Chem. 277 (2002) 6813–6821.
[30] O. Dafi, L. Berrou, Y. Dodier, A. Raybaud, R. Sauvé, L. Parent, Negatively charged residues in the N-terminal of the AID helix confer slow voltage dependent inactivation gating to $Ca_V1.2$, Biophys. J. 87 (2004) 3181–3192.
[31] C.F. Barrett, R.W. Tsien, The Timothy syndrome mutation differentially affects voltage- and calcium-dependent inactivation of $Ca_V1.2$ L-type calcium channels, Proc. Natl. Acad. Sci. U. S. A. 105 (2008) 2157–2162.
[32] F. Findeisen, D.L. Minor Jr., Disruption of the IS6-AID linker affects voltage-gated calcium channel inactivation and facilitation, J. Gen. Physiol. 133 (2009) 327–343.
[33] G. Bernatchez, D. Talwar, L. Parent, Mutations in the EF-hand motif impair the inactivation of barium currents of the cardiac α_{1C} channel, Biophys. J. 75 (1998) 1727–1739.
[34] F. Van Petegem, D.L. Minor Jr., The structural biology of voltage-gated calcium channel function and regulation, Biochem. Soc. Trans. 34 (2006) 887–893.
[35] S. Hering, S. Berjukow, S. Sokolov, R. Marksteiner, R.G. Weiss, R. Kraus, E.N. Timin, Molecular determinants of inactivation in voltage-gated Ca^{2+} channels, J. Physiol. 528 (2000) 237–249.
[36] Y. Jiang, A. Lee, J. Chen, V. Ruta, M. Cadene, B.T. Chait, R. MacKinnon, X-ray structure of a voltage-dependent K^+ channel, Nature 423 (2003) 33–41.
[37] S.K. Tiwari-Woodruff, C.T. Schulteis, A.F. Mock, D.M. Papazian, Electrostatic interactions between transmembrane segments mediate folding of Shaker K+ channel subunits, Biophys. J. 72 (1997) 1489–1500.
[38] I. Vitko, Y. Cheng, J.M. Arias, Y. Shen, X.-R. Wu, E. Perez-Reyes, Functional characterization and neuronal modeling of the effects of childhood absence epilepsy variants of *CACNA1H*, a T-type calcium channel, J. Neurosci. 25 (2005) 4844–4855.
[39] H. Khosravani, C. Altier, B. Simms, K.S. Hamming, T.P. Snutch, J. Mezeyova, J.E. McRory, G.W. Zamponi, Gating effects of mutations in the $Ca_v3.2$ T-type calcium channel associated with childhood absence epilepsy, J. Biol. Chem. 279 (2004) 9681–9684.
[40] Y. Cheng, J. Lu, H. Pan, Y. Zhang, H. Wu, K. Xu, X. Liu, Y. Jiang, X. Bao, Z. Yao, K. Ding, W.H. Lo, B. Qiang, P. Chan, Y. Shen, X. Wu, Association between genetic variation of CACNA1H and childhood absence epilepsy, Ann. Neurol. 54 (2003) 239–243.
[41] J.E. McRory, J. Hamid, C.J. Doering, E. Garcia, R. Parker, K. Hamming, L. Chen, M. Hildebrand, A.M. Beedle, L. Feldcamp, G.W. Zamponi, T.P. Snutch, The CACNA1F gene encodes an L-type calcium channel with unique biophysical properties and tissue distribution, J. Neurosci. 24 (2004) 1707–1718.
[42] F. Lehmann-Horn, K. Jurkat-Rott, Voltage-gated ion channels and hereditary disease, Physiol. Rev. 79 (1999) 1317–1372.
[43] X.D. Tang, I. Marten, P. Dietrich, N. Ivashikina, R. Hedrich, T. Hoshi, Histidine^{118} in the S2–S3 linker specifically controls activation on the KAT1 channel expressed in Xenopus oocytes, Biophys. J. 78 (2000) (2000) 1255–1269.
[44] R.J.G. Cardnell, D.E.D. Nogare, B. Ganetzky, M. Stern, In vivo analysis of a gain-of-function mutation in the Drosophila eag-encoded K^+ channel, Genetics 172 (2006) 2351–2358.
[45] N. Gamper, O. Zaika, Y. Li, P. Martin, C.C. Hernandez, M.R. Perez, A.Y.C. Wang, D.B. Jaffe, M.S. Shapiro, Oxidative modification of M-type K^+ channels as a mechanism of cytoprotective neuronal silencing, EMBO J. 25 (2006) (2006) 4996–5004.
[46] S. Rezazadeh, H.T. Kurata, T.W. Claydon, S.J. Kehl, D. Fedida, An activation gating switch in Kv1.2 is located to a threonine residue in the S2–S3 linker, Biophys. J. 93 (2007) 4173–4186.
[47] N. Pan, J. Sun, C. Lv, H. Li, J. Ding, A hydrophobicity-dependent motif responsible for surface expression of cardiac potassium channel, Cell. Signal. 21 (2009) 349–355.
[48] L.Y. Jan, Y.N. Yan, A superfamily of ion channels, Nature 345 (1990) 672.